

## Validation of CFD Modeling for Multi-dimensional Effects in Ex-vessel Debris Bed Coolability

Mooneon Lee<sup>a\*</sup>, Jin Ho Park<sup>a</sup>, Hyun Sun Park<sup>a</sup>

*a Division of Advanced Nuclear Engineering, Pohang university of science and technology (POSTECH)  
San 31, Hyoja-dong, Nam-gu, Pohang, Gyeongbuk, Republic of KOREA, 790-784*

*\*Corresponding author: hejsunny@postech.ac.kr*

### 1. Introduction

In the very rare case of an accident in light water reactor (LWR), loss of cooling system would occur core meltdown. In the situation, it is expected that the debris bed would be formed in the lower plenum of reactor vessel and the bottom of the cavity in the containment building. Therefore, quantification of debris bed cooling limitation would play a crucial role for evaluation of corium risk to stabilize and terminate severe accident.

The debris bed itself is an exact feature of two-phase flow in porous media. Therefore, in the early years, researchers had tried to figure out frictional force of two phase flow in porous media, which lead to the 1-D analytical model to evaluate dry-out heat flux(DHF) in porous debris bed [1, 2]. However, for the last decay, it is revealed that even very small amount of liquid inflow into debris bed from bottom or side of debris bed could extend the limitation of cooling dramatically (down comer paper). Therefore, the requirements have risen to evaluate the realistic cooling limit of debris bed with consideration of lateral water inflow. In the sense, multi-dimensional CFD simulations has been tried recently [3-5].

In this research, the CFD simulations were performed with the commercial Fluent CFD package by Ansys Inc. The results from simulations were also compared to the experiments and other simulations [5]. The results show similar trends to the other simulations but it seems that additional mesh and time step dependency tests should be proceeded.

### 2. Methods and Results

In the simulations of debris bed, the dominant factors are two phase drag models in porous media. In this research, we used two different models, which are proposed by Reed and Tung & Dhir (T&D) [2, 6].

The heat transfer models are adopted from boiling heat transfer coefficient of a sphere particle[7] with effective interfacial area considering porosity.

Detailed explanations are described in the following sections.

#### 2.1 Drag force models

The earliest drag force models in the evaluation of DHF started from Ergun's model [8], which is semi-empirical model to describe drag force between particle-

fluid in single phase flow. It is later modified by several researchers [1, 2], for consideration of two phase flow effects.

$$\vec{F}_{pi} = \varepsilon \alpha_i \left( \frac{\mu_i}{K_{ri}} \vec{j}_i + \frac{\rho_i}{\eta_{ri}} |\vec{j}_i| \vec{j}_i \right) \quad (1)$$

$$K = \frac{\varepsilon^3 d^2}{150(1-\varepsilon)^2} \quad (2)$$

$$\eta = \frac{\varepsilon^3 d}{1.75(1-\varepsilon)} \quad (3)$$

The subscript 'i' means phases, which are gas and fluid, and 'p' means particle.  $\varepsilon$  is porosity,  $\alpha$  is void fraction,  $\mu$  is viscosity and  $\vec{j}$  is superficial velocity of each phase, defined as volume flow rate,  $\vec{Q}$  (m<sup>3</sup>/s) divided by area (m<sup>2</sup>). In addition,  $K$  and  $\eta$  are permeability and passability, respectively, which are suggested by Ergun.  $K_r$  and  $\eta_r$  are relative permeability and relative passability, respectively, which are functions of void fraction implementing two phase effectiveness. The most common type of their forms are

$$K_{ri} = \alpha_i^n \quad (4)$$

$$\eta_{ri} = \alpha_i^m \quad (5)$$

The powers of void fraction, which are  $n$  and  $m$ , are different for each models. Lipinski suggested 3 for both, and Reed used 3 for  $n$  but 5 for  $m$ .

Later, Tung & Dhir suggested a more detailed model taking account the effectiveness of flow regimes and interfacial drag force between liquid and gas.

$$K_{rg} = \left( \frac{1-\varepsilon}{1-\varepsilon\alpha} \right)^{4/3} \alpha^l, \quad \eta_{rg} = \left( \frac{1-\varepsilon}{1-\varepsilon\alpha} \right)^{2/3} \alpha^l \quad (6)$$

$$K_{rl} = (1-\alpha)^4, \quad \eta_{rl} = (1-\alpha)^4 \quad (7)$$

$$\vec{F}_i = A(\alpha) \vec{j}_r + B(\alpha) |\vec{j}_r| \vec{j}_r \quad (8)$$

Where  $l$  in (6),  $A(\alpha)$  and  $B(\alpha)$  in (8) are various according to flow pattern. The detailed formulations and information about flow patterns are to be taken from [6].

Considering drag forces (1), (8), the time independent momentum equations can be written as

$$-\nabla p_g = \rho_g \vec{g} + \frac{\vec{F}_{pg}}{\varepsilon \alpha} + \frac{\vec{F}_i}{\varepsilon \alpha} \quad (9)$$

$$-\nabla p_l = \rho_l \vec{g} + \frac{\vec{F}_{pl}}{\varepsilon(1-\alpha)} - \frac{\vec{F}_i}{\varepsilon(1-\alpha)} \quad (10)$$

## 2.2 1-D analytical model

In the 1-D steady state mass conservation equations for two phase flow in porous media with phase change are

$$\rho_g \frac{dj_g}{dz} = \Gamma \quad (11)$$

$$\rho_l \frac{dj_l}{dz} = -\Gamma \quad (12)$$

Where  $\Gamma$  is evaporation rate ( $\text{kg}/\text{m}^3\text{s}$ ). In the steady-state conditions for a top flooded bed, the superficial velocity of each phases can be easily derived from (11), (12) by integrating, which leading to

$$j_g = \frac{\ddot{q}z}{\rho_g \Delta H_{\text{evap}}} \quad (13)$$

$$j_l = -\frac{\ddot{q}z}{\rho_l \Delta H_{\text{evap}}} \quad (14)$$

Where  $\ddot{q}$  is volumetric heat generation ( $\text{W}/\text{m}^3$ ) and  $\Delta H_{\text{evap}}$  is latent heat ( $\text{J}/\text{kg}$ ). The heat flux,  $\ddot{q}$  ( $\text{W}/\text{m}^2$ ), is then defined as  $\ddot{q}$  multiplied by height  $z$ (m).

In addition, from equations (9) and (10) with elimination their pressure gradient terms, the momentum balance equation can be expressed as below in the steady state with assumption that there is no pressure difference between fluid and gas phases.

$$(\rho_l - \rho_g) \vec{g} = \frac{\vec{F}_{pg}}{\varepsilon \alpha} - \frac{\vec{F}_{pl}}{\varepsilon(1-\alpha)} + \frac{\vec{F}_i}{\varepsilon \alpha} + \frac{\vec{F}_i}{\varepsilon(1-\alpha)} \quad (15)$$

Once heat flux is determined, the only unknown parameter is a void fraction. Therefore, by the solving the equation (15), void fraction profile depending on the height can be achieved in the steady state.

## 2.3 CFD governing equations

There are two kinds of CFD formulations to simulate fluid flow in porous media, which are the physical velocity and the superficial velocity formulations. Both approaches are available in Fluent 15.0 [9]. The former one is computationally more difficult to solve, especially when the velocity change across the boundary of porous media significantly or the medium is hydro dynamically anisotropic. On the other hand, the latter one is relatively easier to solve and computationally cheaper as there is no change in the superficial velocity across porous media. In addition, the superficial velocity formulation does not take porosity into account when calculating the convection and diffusion terms in the transport equations, which lead numerically significantly more stable but resulting loss of a little of details. In the case of debris bed, as the dominant terms in the momentum balance equations are drag forces caused by porous media [3, 5], we conducted simulations with superficial velocity formulations for quicker convergence and stabilization.

### 2.3.1 Mass conservation equations

In the Fluent 15.0, the mass conservation equations of 2 phase flow in porous media with superficial velocity formulations[5] are

$$\frac{\partial}{\partial t} (\alpha_i \rho_i) + \nabla \cdot (\alpha_i \rho_i \vec{j}_{i,FL}) = \Gamma_i \quad (16)$$

Where  $\vec{j}_{i,FL}$  is the superficial velocity which Fluent uses and is defined somewhat differently to conventional concepts. They did not consider the two phase effect in the superficial velocity, which lead to define as

$$\vec{j}_{i,FL} = \frac{\vec{Q}}{\alpha_i A} = \frac{\vec{j}_i}{\alpha_i} \quad (17)$$

In addition,  $\Gamma_i$  is the evaporation rate achieved from phase change heat transfer rate dividing by latent heat of each phase, which will be discussed later.

$$\Gamma = \frac{Q_{s,sat}}{h_g - h_l} \quad (18)$$

### 2.3.2 Momentum conservation equations

The momentum equations with superficial velocity formulations [5] in Fluent 15.0 are

$$\begin{aligned} & \frac{\partial}{\partial t} (\alpha_i \rho_i \vec{j}_{i,FL}) + \nabla \cdot (\alpha_i \rho_i \vec{j}_{i,FL} \vec{j}_{i,FL}) \\ & = -\alpha_i \vec{\nabla} p_i + \alpha_i \rho_i \vec{g} + \frac{\vec{F}_{s,i}}{\varepsilon} + \frac{\vec{F}_i}{\varepsilon} \end{aligned} \quad (19)$$

The drag forces, which are  $F_{pg}$ ,  $F_{pl}$ ,  $F_i$ , are implemented as same as Reed, and T&D models through UDF. In addition, as the drag models were obtained with considerations of stress term, the stress terms are ignored in this simulation.

### 2.3.3 Energy conservation equations

In the Fluent 15.0, energy conservation equations for two phase porous media[5] are

$$\begin{aligned} & \frac{\partial}{\partial t} (\alpha_i \rho_i h_i) + \nabla \cdot (\alpha_i \rho_i \vec{j}_{i,FL} h_i) \\ & = \nabla \cdot (\lambda_{\text{eff},i} \nabla T_i) + Q_{s,i} + Q_{\text{evap},i} \end{aligned} \quad (20)$$

Where  $h_i$  is an enthalpy of each phase, and  $\lambda_{\text{eff},i}$  is an effective thermal conductivity defined as  $\lambda_{\text{eff},i} = \varepsilon \alpha_i \lambda_i$ .  $Q_{s,i}$  is heat transfer between solid phase in debris bed and fluids. Finally,  $Q_{\text{evap},i}$  is volumetric heat to evaporate.

By default, Fluent 15.0 assumes thermal equilibrium between solid porous medium and fluids, leading no energy exchange terms from solid phase. Therefore, solid phase energy conservation equation was implemented by user-defined scalar transport into Fluent and the equation can be written as

$$\frac{\partial}{\partial t}((1-\varepsilon)\rho_s h_s) = \nabla \cdot (\lambda_{\text{eff},s} \nabla T_s) + Q_{s,\text{decay}} - Q_{s,g} - Q_{s,l} - Q_{s,\text{evap}} \quad (21)$$

In this research, we only considered long term coolability, which do not contain film boiling range, therefore, we adopted the Rohsenow correlation [7] as boiling heat transfer coefficient. The correlation is developed for nucleate boiling on sphere particle. Considering porous medium effects, we used interfacial area density as used in MEWA code [10].

### 3. Verification of the CFD simulation

The simulation conducted with the user-defined functions were verified by simulating 2D axis-symmetric geometry with analytical 1-D model.

#### 3.1 Problem definition

The problem is simple 1-D top flooding situation and the detailed physical conditions and material properties are described in table 1.

Table I: 1D simulation conditions and material properties

Quantity (symbol)	Value (unit)
Pressure (p)	1.0 bar
Bed particle diameter (d)	9.9 mm
Bed porosity( $\varepsilon$ )	0.4
Bed particle density ( $\rho_s$ )	4200 kg/m <sup>3</sup>
Liquid density ( $\rho_l$ )	958.5 kg/m <sup>3</sup>
Gas density ( $\rho_g$ )	0.59 kg/m <sup>3</sup>
Dynamic viscosity for liquid ( $\mu_l$ )	0.0002829
Dynamic viscosity for gas ( $\mu_g$ )	0.0000121
Specific heat capacity for bed ( $c_{p,s}$ )	775.0 J/kgK
Specific heat capacity for liquid ( $c_{p,l}$ )	4216J/kgK
Specific heat capacity for gas ( $c_{p,g}$ )	2024J/kgK
Thermal conductivity for bed ( $\lambda_s$ )	2.0W/Km
Thermal conductivity for liquid ( $\lambda_l$ )	0.681W/Km
Thermal conductivity for gas ( $\lambda_g$ )	0.02466W/Km

The dimension of geometry is a 2D axisymmetric cylinder with radius of 45cm and height of 60cm. The single grid size is about 2 cm x 2 cm. The boundary condition of top surface is pressure outlet and others are set as adiabatic wall condition. The calculations were conducted with 50ms of time step.

#### 3.2 Comparisons between CFD and analytic model

The Fig. 1 shows the heat flux with its maximum void fraction for the Reed and the Tung & Dhir models. The maximum heat flux in the analytic models mean the DHF. Overall, the simulation results from Fluent fits well with the Analytic results except T&D model at 1500kW/m<sup>2</sup>. It is thought that liquid saturation of steady state condition is slightly under the criteria of annular flow,

which is 0.26, yielding fluctuation in momentum equation. It can be observed from simulation results in Fig 2. Because of no slip condition, velocity profile near the wall is distorted. This results slightly higher liquid saturation profile to the center region. Consequently, the void fraction at the top of geometry is fluctuating since the void fraction is changing in between the criteria of annular and annular-slug transition regimes in T&D model.

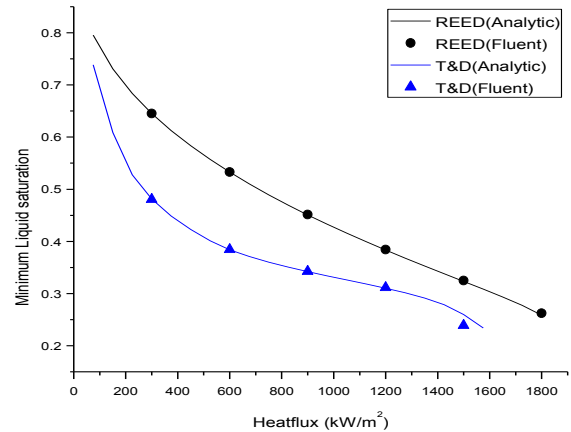


Fig. 1. Heat flux with corresponding maximum void fractions

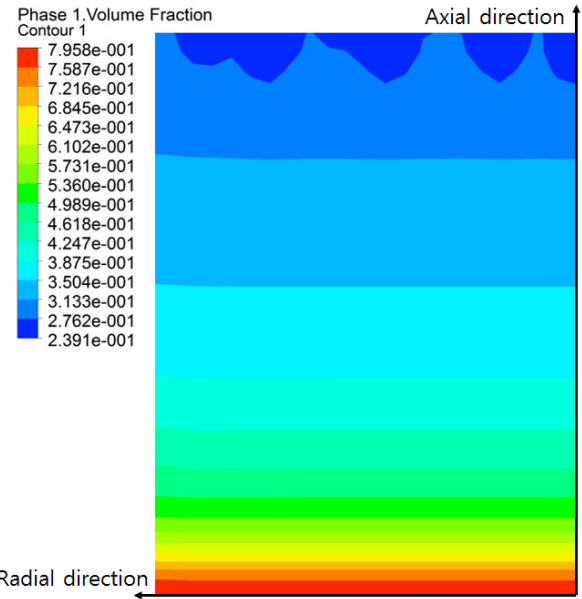


Fig. 2. Saturation profile at 1500kW/m<sup>2</sup> in T&D model.

We also compared other parameters although their DHF values agree well with the analytic solution in the case of 900kW/m<sup>2</sup> in Fig 3-5. The gas superficial velocity and void fraction profile along the height show great agreement to the analytic solution. However, in the case of liquid superficial velocity fluctuating at the top and bottom. According to the Takasuo [5], this is caused by pressure gradient calculation at the wall boundary in the conventional CFD tools. Further study is needed to solve this discrepancy, but it does not affect the results in overall in terms of void fraction profile which represents

dryout condition.

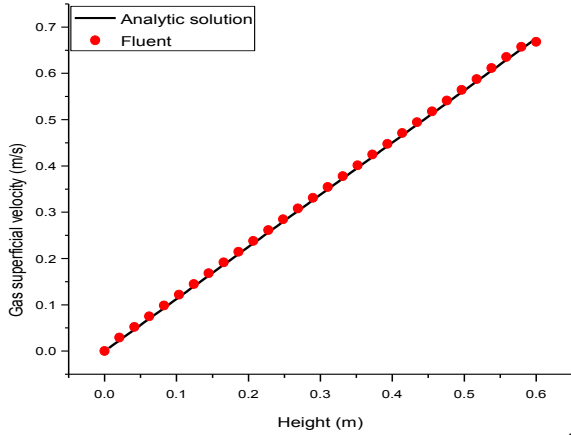


Fig. 3. Height vs vapor superficial velocity in  $900\text{kW/m}^2$  in Reed model

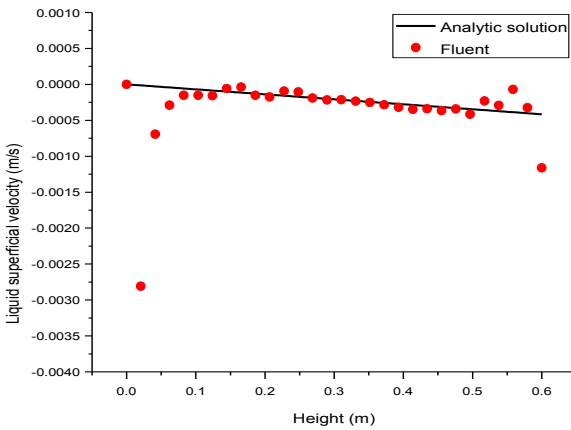


Fig. 4. Height vs liquid superficial velocity in  $900\text{kW/m}^2$  in Reed model

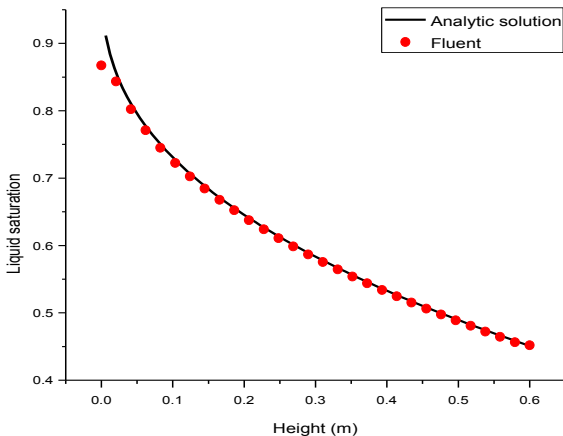


Fig. 5. Height vs void fraction in  $900\text{kW/m}^2$  in Reed model

## 4. Validation with the COOLOCE-10 experiment

### 4.1 Experiments description

The COOLOCE project has been conducted in VTT [5] and designed to evaluate the effectiveness of debris

bed geometry and multi-dimensional effects. They have conducted with various shapes of debris bed including cone, cylinder and mound-shape. In this research, we simulated cylindrical shaped bed, COOLOCE-10, allowing lateral water ingression.

The dimension of debris bed in the COOLOCE-10 is 305mm in diameter and 270mm in height. The test particles are consisted of spherical zirconia/silica beads which sizes are 0.97mm. The porosity of test beds are 0.392. The  $\phi 6.3\text{mm}$  cartridge heaters with 230mm in height are used to simulate decay power with careful configuration for uniform power distribution.

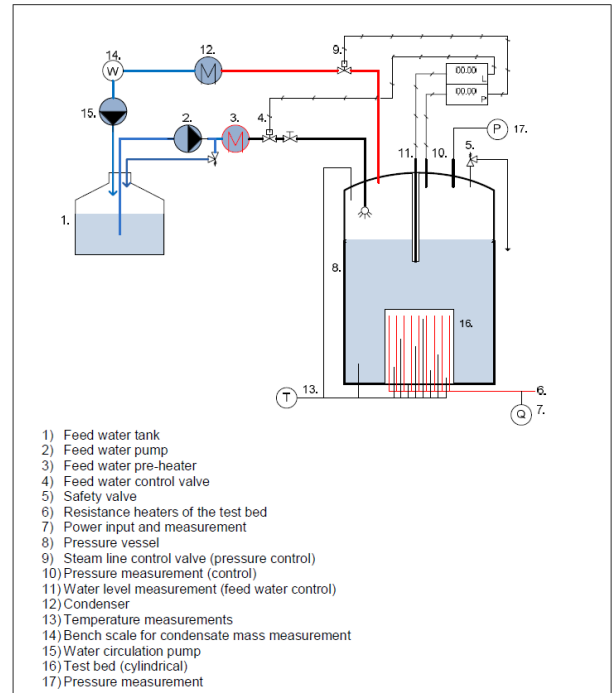


Fig. 6. Schematic flow chart of the COOLOCE test facility [11]

### 4.2 Simulation details

In the Fluent simulation, we used same geometry of debris bed as the one proceeded in experiment and the diameter of water pool surrounding of debris bed is set as 600mm with 450mm in height. The water and steam properties are used from NIST standard reference data[12]. The other properties are listed below in table 2.

Table II: 2D simulation conditions

Quantity (symbol)	Value (unit)
Pressure (p)	1.3-2.93 bar
Bed particle diameter (d)	0.97 mm
Bed porosity( $\epsilon$ )	0.392
Bed particle density ( $\rho_s$ )	4200 kg/m <sup>3</sup>
Specific heat capacity for bed ( $c_{p,s}$ )	775.0 J/kgK
Thermal conductivity for bed ( $\lambda_s$ )	2.0W/Km

Grid cell size	5mm x 5mm
Time step size	100ms
Heating method	Homogeneous
Boundary condition (Top)	Pressure outlet, saturated water inflow
Boundary conditions (Others)	Adiabatic wall
Numerical scheme	Pressure velocity coupled scheme, Least squares cell based, 2 <sup>nd</sup> upwind for momentum, and 1 <sup>st</sup> upwind for others.

All calculations are started from the non-dryout condition and heated up every 300s with 0.025 MW/m<sup>3</sup>. In many cases, especially under dryout condition, the 300s of simulation time is enough to achieve quasi steady state, but longer time needed near and over dryout condition. Therefore, if the maximum temperature of solid phases are not reached to the steady state in 300s, the calculation time is extended until the value does not change along time step.

#### 4.3 Results

As shown in Fig. 7, the trends of dryout powers are well matched to the experiments and simulations in MEWA code [5].

In the cases of Reeds models with 1.3 and 2 bar conditions, the CFD calculation results well match to the MEWA code, with under 0.5% errors, and experiment results, with under 3.3% errors. On the other hand, other cases have errors from 4~8.4% comparing to the results in MEWA code. It is thought that those discrepancy comes from different time steps and numerical schemes between MEWA and Fluent calculations. Therefore, sensitivity tests for those parameters should be conducted in the future.

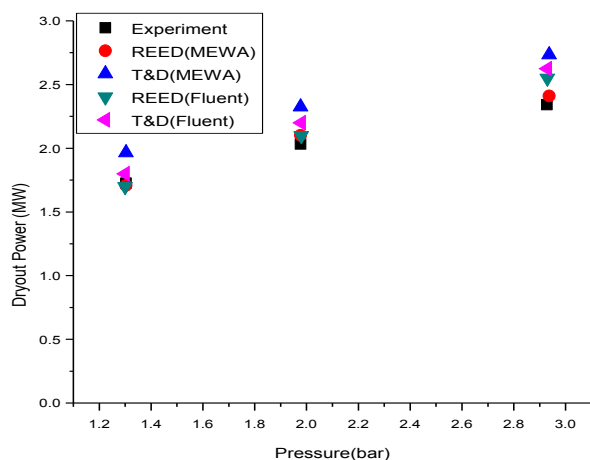


Fig. 7. Dryout power of experiments and simulations

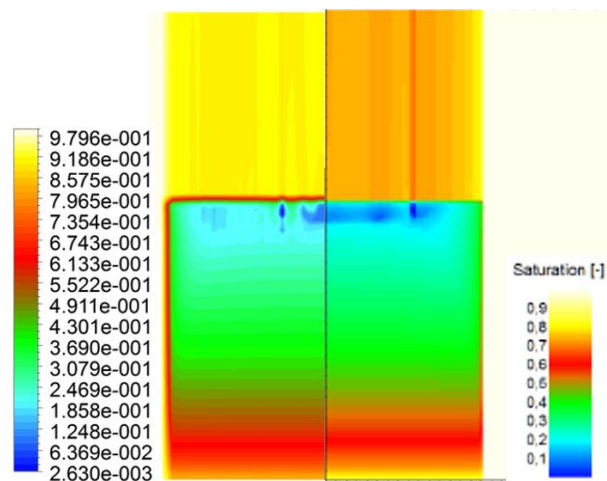


Fig. 8. Comparison of saturation profiles in MEWA and Fluent.

## 5. Conclusions

In this research, we developed user defined function in Fluent 15.0 to simulate ex-vessel debris bed coolability. The user defined functions are verified by 1-D analytic models and they shows good agreements in terms of its dry out condition and liquid saturation profiles.

Following validation processes with 2D geometry with COOLOCE-10 experiments are also conducted and the Fluent calculations show similar trends to the experiments and previous simulations in literature with MEWA code.

On the other hand, analysis on the cases having relatively high discrepancy on the 2D results should be proceeded. In the next step of the research, further sensitivity tests with different time steps and numerical schemes will be conducted.

## ACKNOWLEDGEMENTS

This research was supported by Nuclear Safety Research Program of the Korea Radiation Safety Foundation grants funded by Korean government (NSSC) (Grant Code: 1305008-0113-HD140).

## REFERENCES

- [1] Lipinski, R.J., Model for boiling and dryout in particle beds.[LMFBR]. 1982, Sandia National Labs., Albuquerque, NM (USA).
- [2] Reed, A.W., The effect of channeling on the dryout of heated particulate beds immersed in a liquid pool. 1982, Massachusetts Institute of Technology.
- [3] Bürger, M., et al., Validation and application of the WABE code: Investigations of constitutive laws and 2D effects on debris coolability. Nuclear engineering and design, 2006. 236(19): p. 2164-2188.
- [4] Yakush, S. and P. Kudinov. Effects of water pool subcooling on the debris bed spreading by coolant flow. in ICAPP2011: Proceedings of the 2011 international congress on

advances in nuclear power plants. 2011. American Nuclear Society.

[5] Eveliina Takasuo, V.T., Ville Hovi, A study on the coolability of debris bed geometry variations using 2D and 3D models., in NKS report. 2014: Denmark.

[6] Tung, V.X., Hydrodynamic and thermal aspects of two-phase flow through porous media. 1988, California Univ., Los Angeles, CA (USA).

[7] Rohsenow, W.M., A method of correlating heat transfer data for surface boiling of liquids. 1951, Cambridge, Mass.: MIT Division of Industrial Cooperation,[1951].

[8] Ergun, S., Fluid flow through packed columns. Chemical engineering progress, 1952. 48.

[9] ANSYS, I., ANSYS Fluent User's Guide. 2013, Canonsburg, PA: ANSYS, Inc.

[10] Rahman, S., Coolability of corium debris under severe accident conditions in light water reactors. 2013.

[11] Eveliina Takasuo, T.K., Stefan Holmstrom, Taru Lehtikuusi, COOLOCE debris bed experiments and simulations investigating the coolability of cylindrical beds with different materials and flow modes. NKS reports. 2013, Denmark.

[12] P.J. Linstrom and W.G. Mallard, Eds., NIST Chemistry WebBook, NIST Standard Reference Database Number 69, National Institute of Standards and Technology, Gaithersburg MD, 20899, <http://webbook.nist.gov>, (retrieved August 27, 2015).